AJNR

MR imaging of spinal dysraphism.

N R Altman and D H Altman

AJNR Am J Neuroradiol 1987, 8 (3) 533-538
http://www.ajnr.org/content/8/3/533

MR Imaging of Spinal Dysraphism

Nolan R. Altman[1]
Donald H. Altman

Spinal dysraphism includes anomalies of midline fusion involving bony, mesenchymal, and neural elements. MR imaging of the spine was performed as the initial imaging technique to determine its role in the evaluation of 31 children when spinal dysraphism was clinically suspected or when radiographs revealed errors of ossification of the posterior elements (spina bifida). Correlation of surgical findings in 17 of 18 abnormal examinations and metrizamide myelography with CT in six of these cases indicated that accurate diagnosis was provided by MR in all instances. Examples of spina bifida aperta (spina bifida cystica)—including myelomeningocele, myelocystocele, and lipomyelomeningocele—and those of occult spinal dysraphism—such as dorsal dermal sinus, spinal lipoma, and tight filum terminale (thickened filum)—are presented. These cases show MR to be a reliable technique in the initial evaluation of these disorders.

MR imaging in children with clinically and/or radiographically suspected spinal dysraphism offers a noninvasive technique for evaluating the spine. This procedure can provide a definitive diagnosis without the hazards of ionizing radiation or intrathecal injection of contrast media. Although plain radiographs are helpful in the diagnosis of spina bifida, patients with significant underlying disease can have normal-appearing spines [1]. Metrizamide myelography with CT (MCT) has also been used to evaluate these disorders [2]. Our studies compare these techniques and suggest that MR may be the examination of choice in these entities.

Subjects and Methods

Thirty-one children, ranging in age from 2 days to 14 years, were evaluated with 35 examinations (three patients with two examinations and one with three examinations) from July 1985 through May 1986. All patients received plain radiographs of the spine. MR examinations were correlated with MCT in six cases. Surgical correlation was provided in 17 cases.

The MR was performed with a 0.3-T Fonar B 3000 M MR scanner with a proton resonance frequency of 12.9 MHz. Spin-echo techniques were used with an echo time (TE) of 28 msec and a repetition time (TR) ranging from 300–500 msec. This resulted in T1-weighted images that, with familiarity, were frequently all that were required. The slice thickness was 2 mm with a 0.5-mm interval on the sagittal images. The in-plane spatial resolution was 1 mm. Axial and coronal images were also obtained with a 5-mm slice thickness and a 2-mm interval. In-plane spatial resolution was 0.75 mm. When T2-weighted images were required, a double-echo pulse sequence with a TE of 42 and 84 msec and a TR of 2039 msec was used. The slice thickness was 4 mm with a 1-mm interval. The number of levels was 384 for T1-weighted images and 310 for T2-weighted images along the phase encoding gradient. The frequency encoding gradient was 256.

A 25-cm diameter RF head coil was used in all children who could be placed supine within it. The 25-cm diameter RF body surface coil, which could be wrapped around the body, was used on larger children.

Three- to five-slice axial and coronal plane T1-weighted pulse sequences were initially obtained for localization. The multislice 2-mm-thick sagittal images were obtained either in

Received June 6, 1986; accepted after revision October 8, 1986.

Presented at the annual meeting of the Society for Pediatric Radiology, Washington, DC, April 1986.

[1] Both authors: Department of Radiology, Miami Children's Hospital, 6125 SW 31st St., Miami, FL 33155. Address reprint requests to N. R. Altman.

AJNR 8:533–538, May/June 1987
0195–6108/87/0803–0533

the true sagittal plane or slightly off the sagittal plane as determined from the preliminary scout sequences. Additional axial or T2-weighted images were then obtained if needed. The examinations took from 45–120 min to perform. Visual and cardiac monitoring were obtained on the patients who required sedation. Sedation was usually required for MR and CT on patients between 1 month and 4 years of age. Sedation consisted of chloral hydrate 50 mg/kg orally in children up to 6 kg; for children over 6 kg, Demerol (meperidine) 2 mg/kg, Phenergan 1 mg/kg, and Thorazine 1 mg/kg was used.

Correlative MCT was performed with a GE 8800 scanner. Bone algorithm targeting factors were employed with a magnification factor of two.

Results

A summary of our 31 patients evaluated for spinal dysraphism appears in Table 1. The plain radiograph findings are also correlated with the MR examination in Table 2. It should be noted that the normal plain radiographs in the five cases that had abnormal MR had either associated soft-tissue masses (three cases) or cutaneous markers (two cases). However, several children with severe abnormalities of ossification and segmentation had normal MR examinations (Fig. 1).

The spinal dysraphisms may be divided into occult spinal dysraphism and spina bifida aperta [3]. The occult spinal dysraphism, or the primary tethered cord syndrome [4], designates that group of skin-covered disorders without exposed neural tissue or cystic masses. These disorders are often heralded by cutaneous markers, soft-tissue masses, or neurologic symptoms. MR correctly identified normal from abnormal spinal cord morphology in our cases. The normal filum terminale should be no greater than 1–1.5 mm in thickness and the conus medullaris no lower than the L2 vertebral body [5]. With thin-section sagittal MR, the thickened filum can be identified accurately (Fig. 2). Other entities can also tether the conus below the L2 vertebral body. A lipoma, extending from the subcutaneous fat into the spinal canal with tethering of the cord, is shown in Fig. 3. This is a form of lipomyeloschisis described by Naidich et al. [6]. Note that the spinal cord elements are not involved within the fatty mass, just tethered. The area of low signal intensity is a small amount of cartilage contained within the mass. Follow-up examination revealed release of the cord, and only a small amount of residual lipoma was seen. Another entity that can cause tethering of the conus is a dorsal dermal sinus (Fig. 4). This extended from a cutaneous hemangioma in the sacral region through a bifid sacral spinous process, through the canal to the conus, with tethering. This cephalad ascent of the dermal sinus is typical and is explicitly demonstrated by MR.

TABLE 1: Summary of Cases

Findings	No. of Patients
Myelomeningocele	10*
Lipomyelomeningocele	2*
Meningocele	1*
Myelocystocele	1*
Lipoma	1*
Thickened filum	1*
Dorsal dermal sinus	1*
Caudal regression	1
Normal	13
Total	31

* Surgical pathology correlation.

TABLE 2: Correlation of MR and Plain Radiograph Findings

Findings	No. of Patients
Normal MR	13
Normal plain radiograph	10
Abnormal plain radiograph	3
Abnormal MR	18
Normal plain radiograph	5
Abnormal plain radiograph	13
Total	31

The second group of disorders, the spina bifida aperta (cystica), are designated by posterior protrusion of all or part of the spinal contents through a posterior spina bifida. MR is an easy way to demonstrate these disorders, which present at birth (Fig. 5). The myelomeningocele of the lumbosacral region is the most common. This is repaired at birth and usually does not re-present until there is a growth spurt, when the tethering of the cord secondary to the neural placode becomes clinically significant. Other less common areas are in the cervical region (Fig. 6), where the neural placode can be seen in association with the Chiari II malformation, and in the thoracic region without a neural placode, thereby representing a meningocele (Fig. 7).

More complicated disorders can occur when there is cystic dilatation of the terminal portion of the spinal cord from CSF; hence, a myelocystocele (Fig. 8). In the more proximal portion of the cord, cystic dilatation represents a hydromyelia. Postoperative MR shows drainage of the myelocystocele via a lumbar peritoneal shunt; however, the hydromyelia persists.

A lipomyelomeningocele is the second form of lipomyeloschisis described by Naidich et al. [6]. The fatty mass that involves neural elements outside the spinal canal is well seen on the sagittal plane (Fig. 9A). The degree of rotation of the neural placode is seen better on the axial images (Fig. 9B).

In our cases, MR accurately demonstrated these disorders as compared with MCT and surgical findings. Of the 31 patients examined, 18 were determined to be abnormal by MR. Seventeen of these were surgically evaluated, and those findings correlated with the MR results. The case of caudal regression was the only abnormal case not surgically proven. Six of the 18 abnormal cases were also evaluated by MCT, including the cases of lipoma (Fig. 3), dorsal dermal sinus (Fig. 4), myelocystocele (Fig. 8), lipomyelomeningocele (Fig. 9), and two cases of myelomeningocele. In these cases, we think MR demonstrated the abnormalities as well as MCT did. In addition, in the case of the myelocystocele, MR was the only technique that demonstrated the dilated cystic portion of the cord, thereby making the diagnosis. It also provided a noninvasive way to follow up.

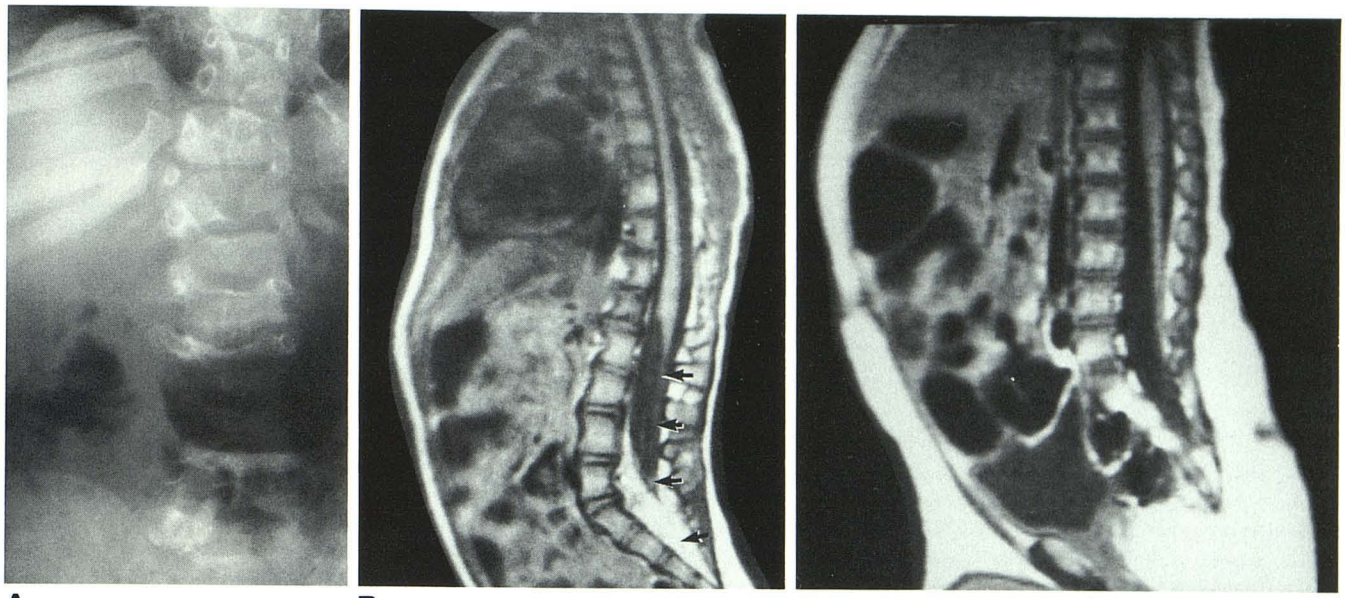

Fig. 1.—Multiple segmentation and ossification abnormalities with a normal cord.
***A*, Radiograph demonstrating multiple segmentation and ossification abnormalities of spine.**
***B*, Sagittal T1-weighted MR shows normal level of tip of conus medullaris at L2 vertebral body level. Normal-appearing filum terminale is shown posteriorly within thecal sac, piercing dura, traversing epidural fat, and attaching to dorsal aspect of first proximal sacrococcygeal segment (*arrows*). Note that normal cord is of intermediate signal intensity while CSF appears to be of low signal intensity due to long T1 relaxation. Epidural fat, which can be quite variable in amount at caudal end of subarachnoid space, shows high signal intensity reflecting a short T1 relaxation.**

Fig. 2.—Thickened filum with tethered cord (tight filum terminale). Sagittal T1-weighted MR shows thickened filum terminale with tethering of conus medullaris.

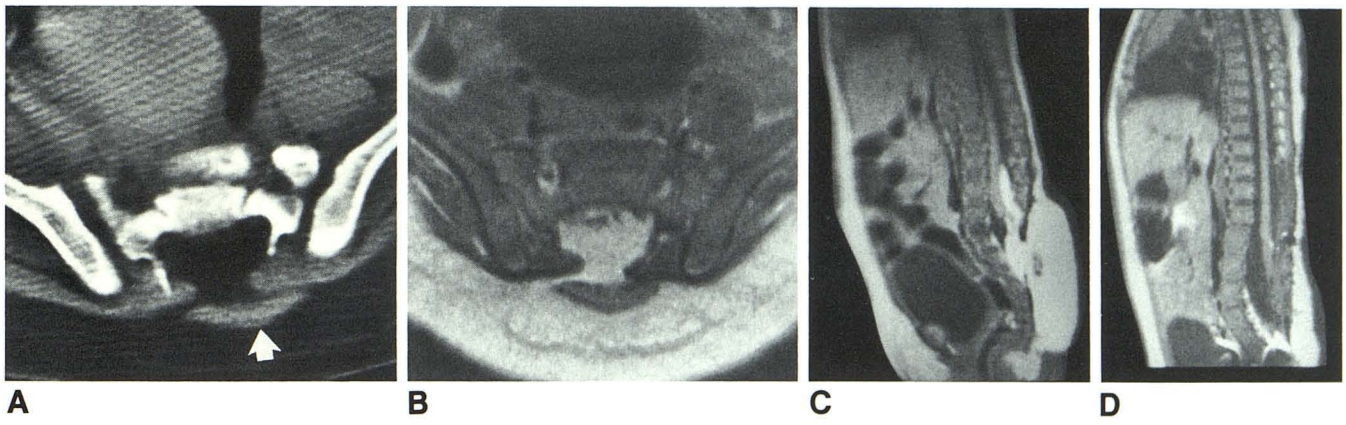

Fig. 3.—Spinal lipoma with tethering of cord (lipomyeloschisis).
***A*, Axial CT demonstrates spina bifida with a widened canal and region of decreased attenuation coefficient contained within canal, representing fat. Soft-tissue density within fat, outside the canal space, represents a small amount of cartilage, found surgically (*arrow*).**
***B*, Axial T1-weighted MR shows high signal intensity reflecting short T1 relaxation of fat, extending from subcutaneous region into canal.**
***C*, Sagittal T1-weighted MR demonstrates tethered cord secondary to spinal lipoma.**
***D*, Sagittal T1-weighted MR postoperative examination shows release of cord and almost complete removal of lipoma.**

Discussion

MR is becoming the technique of choice for evaluating the spines of children with suspected spinal dysraphism. Recent reports also indicate that MR should be the screening technique of choice [7, 8]. We concur with these findings and offer the cases reported here as illustrative of the spectrum of disorders encountered. Two of our cases also demonstrate how easily follow-up can be performed.

With thin sections (2–3 mm) and short TE and TR, produc-

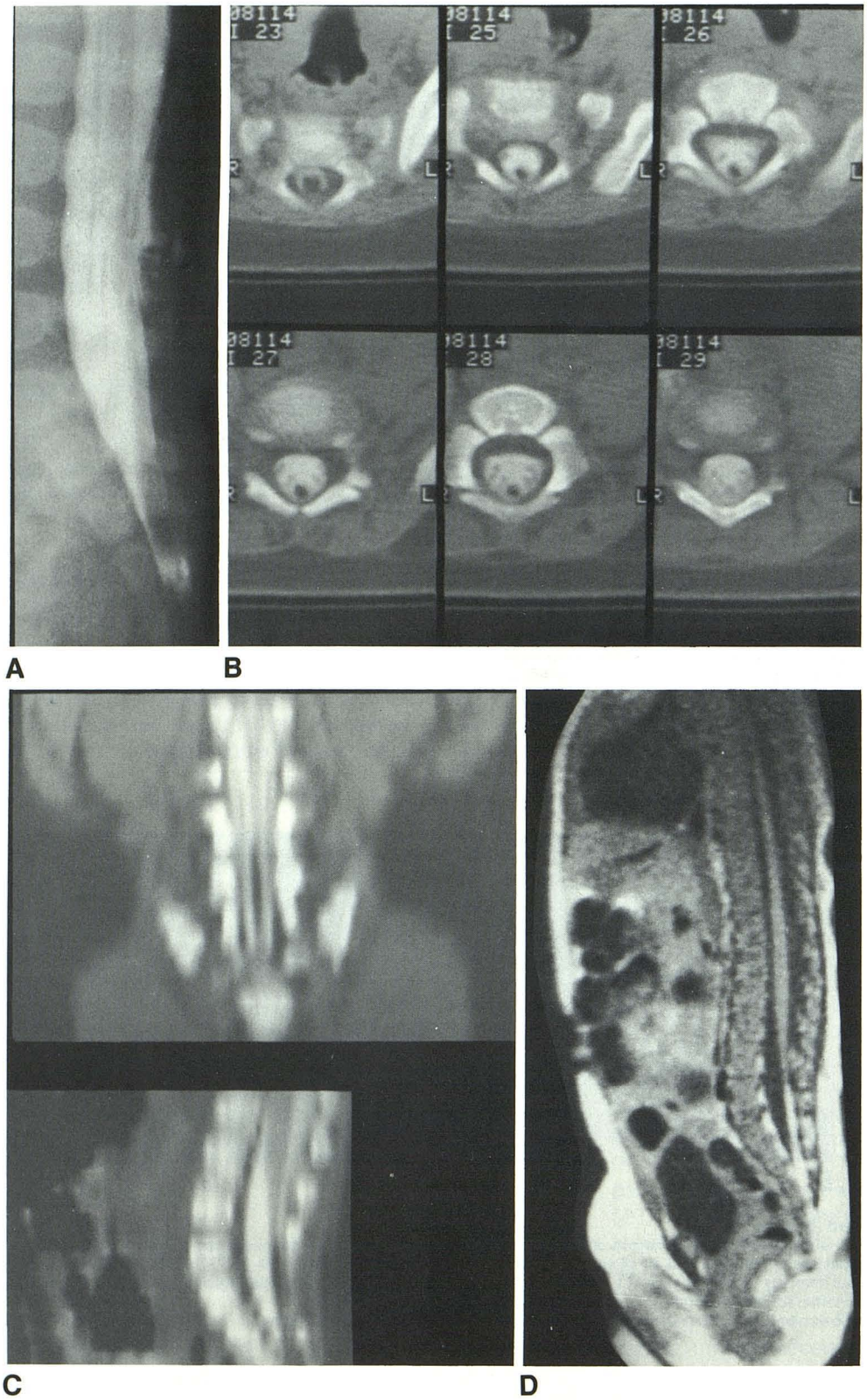

Fig. 4.—Dorsal dermal sinus.

***A*, Lateral metrizamide myelogram radiographs show low position of cord and markedly thickened filum terminale with a caudal mass.**

***B*, Axial metrizamide CT shows an area of low attenuation coefficient, consistent with fat, extending from level of conus, caudally.**

***C*, Reformatted metrizamide CT in coronal and sagittal planes with fatty mass extending to level of conus.**

***D*, Sagittal T1-weighted MR shows sacral dimple of skin and area of high signal intensity reflecting short T1 relaxation of subcutaneous fat, which is identical to mass extending cephalad through thecal sac to conus.**

ing T1-weighted images, predominantly in the sagittal and axial planes, adequate evaluation of the dysraphic spine can be obtained. The only caution is in the case of the thickened filum. Recently, it has been reported that a filum thicker than 1–1.5 mm or a conus lower than the L2 vertebral body is abnormal. MR can easily identify the level of the conus and, with thin sections, it can also identify the filum terminale, as illustrated in our cases. If the MR is normal and a tight filum

Fig. 5.—Lumbosacral myelomeningocele. Sagittal T1-weighted MR demonstrates lumbosacral myelomeningocele. Dorsal extent of neural placode is seen clearly (*arrows*).

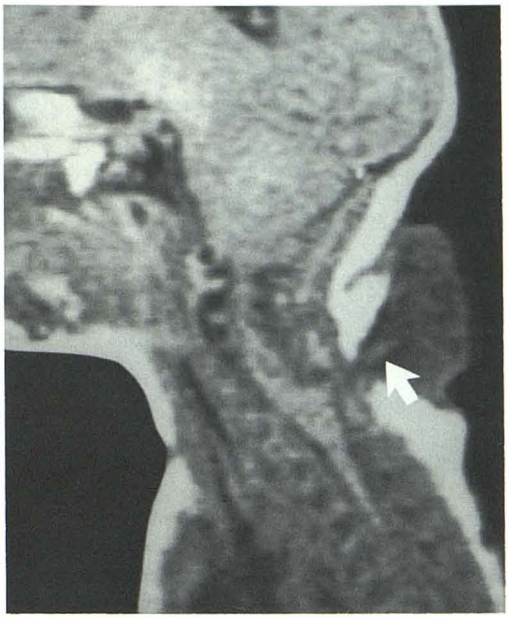

Fig. 6.—Cervical myelomeningocele. Sagittal T1-weighted MR demonstrates neural placode (*arrow*) extending into cervical myelomeningocele. In addition, the associated Chiari II malformation of the brain is demonstrated with low position of posterior fossa contents.

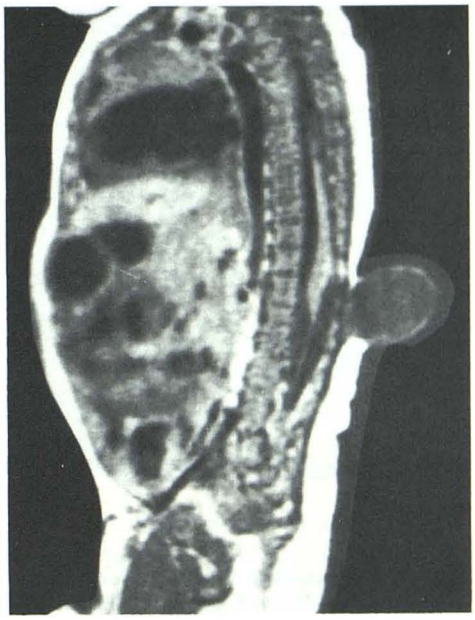

Fig. 7.—Thoracic meningocele. Sagittal T1-weighted MR with thickening of distal portion of cord. No neural elements are contained within meningocele.

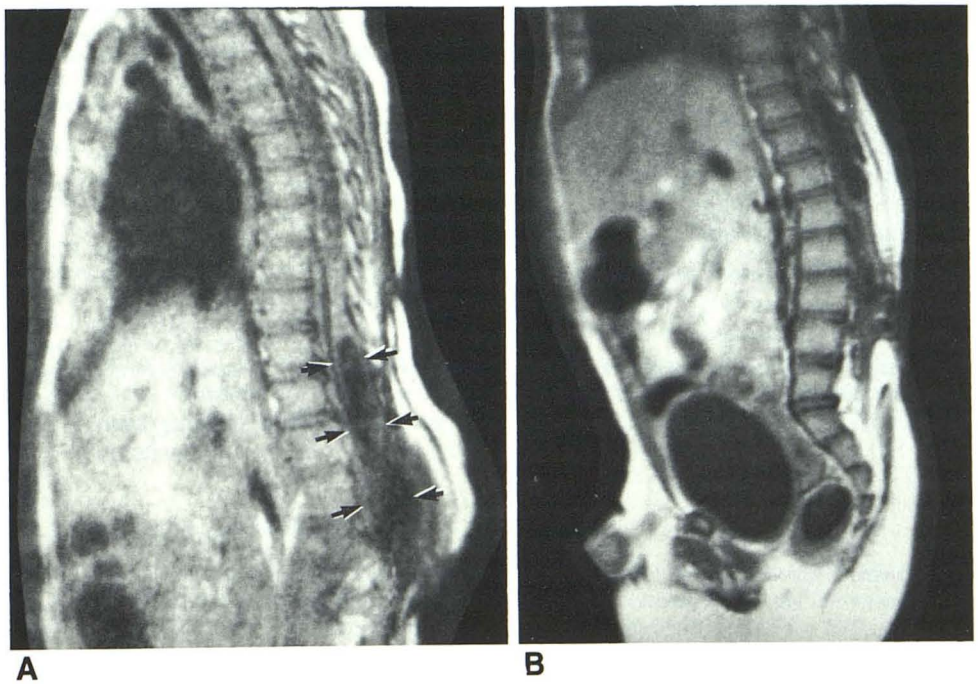

A B

Fig. 8.—Myelocystocele. Sagittal T1-weighted MR with preoperative (*A*) and postoperative (*B*) examinations. On preoperative study, a huge cytic dilatation of distal cord is seen extending through canal space into dorsal soft tissues representing the myelocystocele (*arrows*). Proximally, within cord, there is also cystic dilatation representing a hydromyelia. The postoperative examination still shows the hydromyelia; however, the myelocystocele has been evacuated secondary to lumbar peritoneal shunt placement.

terminale is still suspected clinically, then MCT with plain myelography still offers better spatial resolution. Myelography also offers better visualization of the course of individual nerve roots. This is particularly important if there are vulnerable nerve roots in the proposed surgical field. However, in these cases presented, MR determined feasibility of surgery and, in the cases where MCT and MR were compared, no additional information was gained. MR was actually the only examination to determine the myelocystocele and, thereby, to plan the required lumboperitoneal shunt.

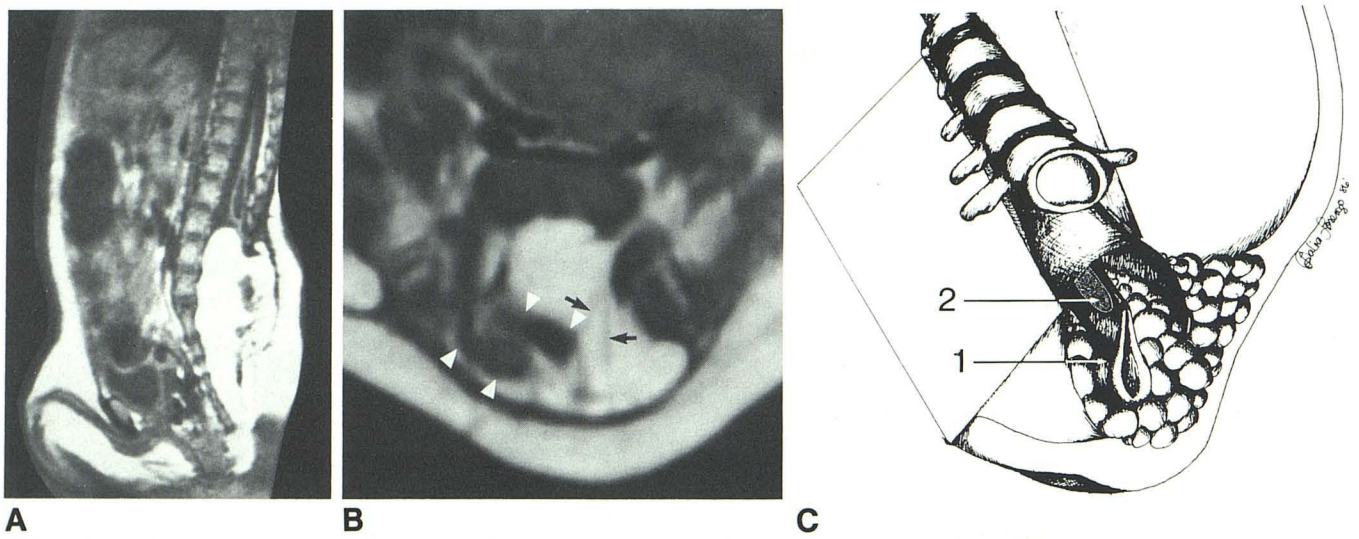

Fig. 9.—Lipomyelomeningocele (lipomyeloschisis).

***A*, Sagittal T1-weighted MR shows dorsal lumbosacral soft-tissue mass with signal intensity corresponding to fat, extending from subcutaneous tissues into canal and tethering of cord. There is a neural placode identified within this mass as evidenced by areas of low signal intensity contained within primarily high signal intensity fatty mass. Also, a distal cystic dilatation within cord is seen representing a hydromyelia.**

***B*, Axial T1-weighted MR again demonstrates neural placode displaced to right in the mass (*arrowheads*). Nerve roots are shown traversing fatty mass toward spinal canal (*arrows*).**

***C*, Diagrammatic representation of this complex anomaly. The neuroplacode (1) and hydromyelia (2) of the lipomyelomeningocele are illustrated.**

The correlation of sonography was not addressed in this study. Since sedation is not required in neonates, the anatomic detail provided by MR was considered to be superior to that which would have been obtained with sonography.

For these reasons, we believe that in the dysraphic disorders, MR should be the initial procedure of choice. The child is not exposed to ionizing radiation and the examination is completely noninvasive, eliminating the need for general anesthesia and intrathecal contrast material. With the use of MR, we believe the need for myelography in the majority of these disorders may be obviated.

REFERENCES

1. Naidich TP, Doundoulakis SH, Poznanski AK. Intraspinal masses: efficacy of plain spine radiography. *Pediatr Neurosci* **1986**;12:10–17
2. Harwood-Nash DC. Computed tomography of the pediatric spine: a protocol for the 1980's. *Radiol Clin North Am* **1981**;19:479–494
3. Naidich TP, Harwood-Nash DC, Milone DG. Radiology of spinal dysraphism. *Clin Neurosurg* **1983**;30:341–365
4. Sarwar M, Virapongse C, Ghimani S. Primary tethered cord syndrome: a new hypothesis of its origin. *AJNR* **1984**;5:235–242
5. Hochhouser L, Chuang S, Harwood-Nash DC, Fitz CR, Armstrong D, Savoie J. The tethered cord syndrome revisited. Presented at the annual meeting of the American Society of Neuroradiology, San Diego, January **1986**. *AJNR* **1986**;7:543 (abstr)
6. Naidich TP, McLone DG, Mutluer S. A new understanding of dorsal dysraphism with lipoma (lipomyeloschisis): radiologic evaluation and surgical correction. *AJNR* **1983**;4:103–116
7. Barnes PD, Lester PD, Yamanashi WS, Prince JR. Magnetic resonance imaging in infants and children with spinal dysraphism. *AJNR* **1986**;7:465–472
8. DeLaPaz RL, Floris R, Norman D, Newton TH. MRI of tethered spinal cord and caudal lipoma. Presented at the annual meeting of the American Society of Neuroradiology, San Diego, January **1986.** *AJNR* **1986**;7:550 (abstr)